

层状高温超导体中约瑟夫森等离子体模式太赫兹二维相干光谱的理论研究

李子龙^{1,2}, 万源^{1,2,3*}

¹中国科学院物理研究所, 凝聚态理论与计算重点实验室, 北京 100190;

²中国科学院大学物理科学学院, 北京 100049;

³松山湖材料实验室, 广东 东莞 523808

摘要 研究了层状高温超导体中约瑟夫森等离子体模式对电场的非线性响应及对应的太赫兹二维相干光谱。从半经典有效模型出发, 推导出了约瑟夫森相位的运动方程。通过求解这一运动方程, 发现太赫兹二维相干光谱中存在“泵浦-探测”信号、回波信号、失相信号和双量子相干信号。进一步将这些信号与刘维尔路径联系起来, 说明体系的具体激发过程, 并借此说明这些信号的潜在应用。

关键词 太赫兹; 太赫兹二维相干光谱; 约瑟夫森等离子体模式; 层状高温超导体

中图分类号 O415 文献标志码 A

DOI: 10.3788/CJL230796

1 引言

强关联体系是指由相互作用极强的电子组成的体系, 包括高温超导体^[1-2]、量子磁体^[3-4]、重费米子体系^[5-6]等。理解并预测强关联体系的性质是凝聚态物理的一个重要课题。光谱学是研究凝聚态体系的一种重要方法。光谱学方法利用电磁波与物质的相互作用探测材料中激发的性质, 其在强关联体系中的应用依赖于电磁波频率与激发能量的匹配。强关联体系中的集体现象的能量尺度多在太赫兹波段, 例如, 高温超导体的赝能隙和超导转变温度对应的能量为几十毫电子伏特^[1-2], 量子磁性材料中的磁激发对应的能量尺度为几个到几十毫电子伏特^[3-4], 重费米子体系的近藤温度多为几十开尔文^[5-6], 这些能量尺度均对应电磁波中的太赫兹波段, 因此太赫兹光谱学^[7]对强关联体系的研究具有重要意义。然而, 微波频段的电磁波能够利用电学手段高效产生, 可见光及其附近频段的电磁波能够通过半导体激光等手段高效产生, 而太赫兹波段刚好处于两种方法的频率窗口之外, 产生高效的太赫兹脉冲面临着巨大的挑战, 这一现象又被称为“太赫兹空隙”^[8]。近些年, 产生太赫兹脉冲的方法逐渐成熟起来^[9-10], 使得太赫兹光谱学在强关联体系中的应用成为可能。

太赫兹线性光谱利用单个太赫兹光脉冲测量材料对电磁波的线性响应, 以此来探测材料中激发的性

质。材料中的不均匀性, 比如杂质和缺陷等, 会为线性光谱引入非均匀展宽。这种非均匀展宽与由激发的寿命和体系的退相干引起的均匀展宽混合在一起, 难以区分^[11-12]。二维相干光谱(2DCS)为这一问题提供了解决方法。太赫兹二维相干光谱利用多个太赫兹相干光脉冲来探测材料的非线性响应, 从而在频域上产生一个二维(多维)光谱^[11-14]。通过选择合适的脉冲序列, 并精确调控脉冲之间的时间间隔, 二维相干光谱上会出现光子回波信号^[15]。这一信号能将均匀展宽和不均匀展宽区分开, 从而得到线性光谱中被隐藏的信息。

当下强关联体系太赫兹二维相干光谱的理论研究主要集中在自旋液体体系中^[16-21]。自旋液体的激发是分数激发, 其线性光谱是由这些分数激发组成的连续谱, 因而激发的寿命和退相干时间等信息都被隐藏了起来。理论研究发现, 二维相干光谱的特征揭示了体系中分数激发的种类及其动力学信息。这些现象说明了太赫兹二维相干光谱在强关联体系中的巨大潜力。与此同时, 无序系统^[22]、非可积系统^[23-24]的二维相干光谱也被进一步研究, 这些体系的二维相干光谱都提供了超越线性光谱的信息。然而, 这些研究大多集中于磁性系统, 相比带电体系, 其与电磁波的耦合强度更弱^[25], 因而较难测量这些体系的太赫兹二维相干光谱。对带电体系的太赫兹二维相干光谱研究有更强的实验相关性。

收稿日期: 2023-05-04; 修回日期: 2023-07-19; 录用日期: 2023-07-21; 网络首发日期: 2023-07-28

基金项目: 国家自然科学基金(12250008)

通信作者: *yuan.wan@iphy.ac.cn

以 $\text{La}_{2-x}\text{Ba}_x\text{CuO}_4$ 、 $\text{Bi}_2\text{Sr}_2\text{Ca}_{n-1}\text{Cu}_n\text{O}_{2n+4+x}$ 等为代表的铜基超导体在高温超导体中占据着重要地位^[1-2]。这些超导体具有层状结构,沿 c 轴超导层和绝缘层交替分布,因而具有约瑟夫森隧穿效应。这种隧穿效应产生了一种高度非线性的模式——约瑟夫森等离子体模式,这一模式的激发频率处于太赫兹波段^[26]。约瑟夫森等离子体模式与库珀对的隧穿联系在一起,因而能够体现超导的形成过程,对于超导研究具有重要意义^[26-27]。鉴于此,最近有实验运用太赫兹光谱学手段测量了 $\text{La}_{2-x}\text{Ba}_x\text{CuO}_4$ 中约瑟夫森等离子体模式的非线性响应^[28]。一个自然的问题是,约瑟夫森等离子体的二维相干光谱的特征是怎样的?针对这一问题,本文做出初步的理论分析。在介绍模型的细节并利用哈密顿方程得到约瑟夫森相位运动方程后,利用格林函数方法和数值方法计算这一运动方程,并得到其对外加电场的非线性响应,然后展示了该体系的非线性响应和太赫兹二维相干光谱的主要结果。

2 模型介绍与运动方程

考虑一个由约瑟夫森结组成的体系。如图 1 所示,超导体被绝缘层分隔开,在超导相,相邻超导体的相位具有约瑟夫森相互作用。在这一相互作用下,一种低能的集体激发为约瑟夫森等离子体模式,其来源于库珀对的隧穿效应,因而能够被电场激发。忽略掉超导相位 ϕ 的量子涨落,在考虑与电场的相互作用时,该模型的半经典哈密顿量写作^[29]

$$H = \frac{\epsilon A d}{2} \sum_j \left[E_{j+\frac{1}{2}} + E(t) \right]^2 - J \sum_j \cos(\phi_j - \phi_{j-1}), \quad (1)$$

式中: ϵ 为绝缘层的电介质常数; A 为绝缘层上下平面的面积; d 为绝缘层的厚度; $E(t)$ 为外加电场; $E_{j+\frac{1}{2}}$ 为 j 层超导体和 $j+1$ 层超导体之间的内建电场; J 为约瑟

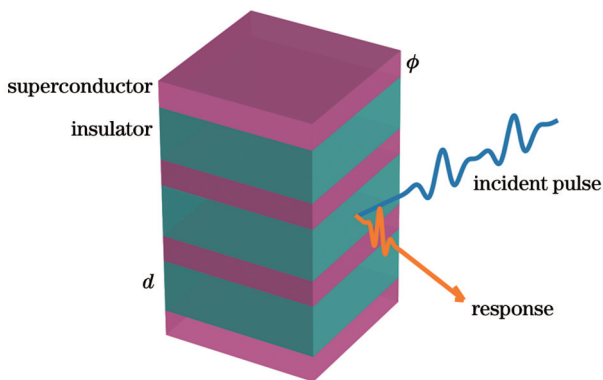


图 1 模型的结构。 d 为绝缘层厚度, ϕ 为超导相位

Fig. 1 Structure of considered model. d represents thickness of each insulator, and ϕ denotes phase of each superconductor

夫森耦合常数。

这一半经典哈密顿量具有明确的物理意义,其中第一项描述了约瑟夫森结的电容效应,第二项描述了超导相位的约瑟夫森相互作用。库珀对隧穿的耗散效应将在稍后唯象地添加。这一模型能够描述铜基超导体 $\text{La}_{2-x}\text{Ba}_x\text{CuO}_4$ (LBCO) 沿 c 轴的特征^[26],其中 CuO_2 对应图 1 中的超导层,相邻超导层被绝缘层分开,共同组成一个约瑟夫森结。在层状高温超导体中,由于超导相干长度远大于超导层厚度,因此可以近似认为超导序参量在层内、沿着厚度方向为一常数。超导层厚度的效应被吸收到了约瑟夫森耦合常数 J 中。

本文主要研究这一体系对电场的非线性响应,并讨论其二维相干光谱的主要特征。

$E_{j+\frac{1}{2}}$ 来源于约瑟夫森结的电容效应。设 j 层超导体的净电荷为 $-eN_j$,按照高斯定律,其内建电场满足

$$E_{j+\frac{1}{2}} - E_{j-\frac{1}{2}} = -\frac{eN_j}{\epsilon A}. \quad (2)$$

利用式(2),我们可以将内建电场表达为

$$E_{j+\frac{1}{2}} = -\sum_{i \leq j} \frac{eN_i}{\epsilon A}. \quad (3)$$

由相位和粒子数 N_i 的量子对易关系^[30]

$$[N_i, \phi_j] = -i\delta_{ij}, \quad (4)$$

得到其经典泊松括号为

$$[N_i, \phi_j]_{\text{PB}} = -\delta_{ij}. \quad (5)$$

联合式(3)和式(5),即得到内建电场与相位之间的泊松括号:

$$[E_{i+\frac{1}{2}}, \phi_j]_{\text{PB}} = \frac{e}{\epsilon A} \theta_{ij}, \quad (6)$$

式中: $i \geq j$ 时 $\theta_{ij} = 1$, $i < j$ 时 $\theta_{ij} = 0$ 。

定义相位差 $\Delta\phi_j = \phi_{j+1} - \phi_j$,内建电场与之的泊松括号为

$$[E_{i+\frac{1}{2}}, \Delta\phi_j]_{\text{PB}} = -\frac{e}{\epsilon A} \delta_{ij}. \quad (7)$$

式(7)说明, $\frac{\epsilon A}{e} E_{i+\frac{1}{2}}$ 与 $\Delta\phi_i$ 共轭。令

$\pi_i = \frac{\epsilon A}{e} E_{i+\frac{1}{2}}$ 以及约瑟夫森相位 $\theta_i = \Delta\phi_i$ 。在这一正则坐标下,不同格点脱耦:

$$H = \sum_j \left\{ \frac{\epsilon A d}{2} \left[\frac{e}{\epsilon A} \pi_j + E(t) \right]^2 - J \cos \theta_j \right\}. \quad (8)$$

正则动量 π_j 和正则坐标 θ_j 的时间演化为

$$\begin{cases} \frac{d\pi_j(t)}{dt} = [\pi_j(t), H]_{\text{PB}} = -J \sin \theta_j \\ \frac{d\theta_j(t)}{dt} = [\theta_j(t), H]_{\text{PB}} = \frac{de^2}{\epsilon A} \pi_j + edE(t) \end{cases}. \quad (9)$$

略去格点的指标,并利用瑞利耗散函数为体系唯

象地加入耗散过程,得到

$$\begin{cases} \frac{d\pi(t)}{dt} = [\pi(t), H]_{\text{PB}} - \frac{\partial R(\dot{\theta})}{\partial \dot{\theta}} = -J \sin \theta - \beta \dot{\theta} \\ \frac{d\theta(t)}{dt} = [\theta(t), H]_{\text{PB}} = \frac{de^2}{\epsilon A} \pi + edE(t) \end{cases}, (10)$$

其中,选择瑞利耗散函数 $R(\dot{\theta}) = \frac{\beta}{2} \dot{\theta}^2$ 。选择这一形式的原因在于, $\dot{\theta}$ 对应着库珀对的隧穿电流,这种瑞利耗散函数体现了由电阻引起的耗散过程。

由式(10)得到 θ 的运动方程:

$$\ddot{\theta} + \Gamma \dot{\theta} + \omega^2 \sin \theta = F(t), (11)$$

式中: $\Gamma = \beta \frac{de^2}{\epsilon A}$; $\omega^2 = J \frac{de^2}{\epsilon A}$; $F(t) = ed\dot{E}(t)$; ω 为约瑟夫森等离子体振荡频率。

式(11)包含了约瑟夫森结的电容效应、电阻效应以及约瑟夫森效应,实际也就是电阻、电容分路结模型(RCSJ模型)在外加电流激励下的运动方程^[29]。我们考虑一种简单的情形,当施加静电场时,即 $E(t) = E$ 时,运动方程有一静态解: $\theta = 0, \pi = -\frac{\epsilon A}{e} E$, 对应于内建电场 $E_{j+\frac{1}{2}} = -E$, 内建电场与外加电场互相抵消,这正是电容器的基本特征。在另一种情形下, $E(t) = \delta(t)$, 在 t 足够大时,体系会回到 $\theta = 0, \pi = 0$ 的状态。这体现了体系中的耗散过程,这是电阻的基本特征。

做变量代换, $\tilde{t} = \omega t, \gamma = \Gamma/\omega$ 以及 $f(t) = F(t)/\omega^2$, 得到式(11)的无量纲形式:

$$\ddot{\theta} + \gamma \dot{\theta} + \sin \theta = f(\tilde{t}). (12)$$

式(12)是本节的主要结果。体系的非线性响应来源于运动方程中的非线性项 $\sin \theta$ 。

3 方 法

驱动项 $f(\tilde{t})$ 较小,即 $\int d\tilde{t} |f(\tilde{t})| \ll 1$ 时, $|\theta| \ll 1$ 。为

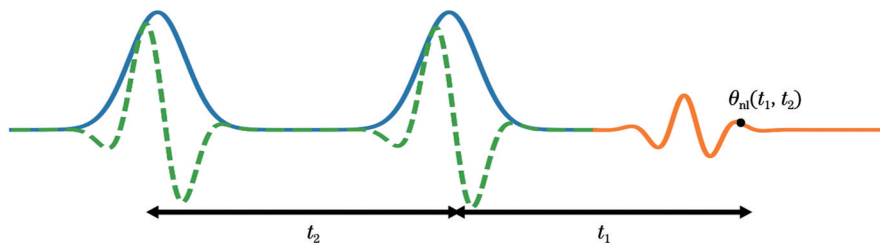


图2 脉冲序列。格林函数方法选取了蓝色曲线所示的入射脉冲序列,数值方法选取了绿色曲线所示的入射脉冲序列。两个脉冲的时间间隔为 t_2 , 测量时间点与第二个脉冲的时间间隔为 t_1

Fig. 2 Pulse sequence. Blue curve represents incident pulse sequence used in Green's function method, and green curve represents incident pulse sequence used in numerical method. Time separation between two pulses is t_2 , and time separation between measurement and the last pulse is t_1

了讨论体系的非线性响应,我们将 $\sin \theta$ 做泰勒展开至第三阶并代入式(12)得到

$$\ddot{\theta} + \gamma \dot{\theta} + \theta - \frac{\theta^3}{6} = f(\tilde{t}). (13)$$

将 θ 按阶展开 $\theta = \theta_{(1)} + \theta_{(2)} + \dots$, 并代入式(13)得到

$$\begin{cases} \left(\frac{d^2}{d\tilde{t}^2} + \gamma \frac{d}{d\tilde{t}} + 1 \right) \theta_{(1)} = f(\tilde{t}) \\ \left(\frac{d^2}{d\tilde{t}^2} + \gamma \frac{d}{d\tilde{t}} + 1 \right) \theta_{(2)} = 0 \\ \left(\frac{d^2}{d\tilde{t}^2} + \gamma \frac{d}{d\tilde{t}} + 1 \right) \theta_{(3)} = \frac{\theta_{(1)}^3}{6} \end{cases}. (14)$$

首先求解以下格林函数:

$$\left(\frac{d^2}{d\tilde{t}^2} + \gamma \frac{d}{d\tilde{t}} + 1 \right) G(\tilde{t}) = \delta(\tilde{t}), (15)$$

解得

$$G(\tilde{t}) = \frac{\Theta(\tilde{t})}{\Delta} \exp\left(-\frac{\gamma}{2} \tilde{t}\right) \sin \Delta \tilde{t}, (16)$$

其中, $\Delta = \frac{\sqrt{4 - \gamma^2}}{2}$ 。

利用格林函数,首先得到 $\theta_{(1)}(\tilde{t})$:

$$\theta_{(1)}(\tilde{t}) = \int_{-\infty}^{\tilde{t}} d\tilde{\tau} G(\tilde{t} - \tilde{\tau}) f(\tilde{\tau}). (17)$$

同样可以得到

$$\begin{cases} \theta_{(2)}(\tilde{t}) = 0 \\ \theta_{(3)}(\tilde{t}) = \int_{-\infty}^{\tilde{t}} d\tilde{\tau} G(\tilde{t} - \tilde{\tau}) \frac{\theta_{(1)}^3(\tilde{\tau})}{6} \end{cases}. (18)$$

我们考虑图2所示的脉冲序列。假设外电场 $E(t)$ 来源于光脉冲,并且其形式可以大致写成 $E(\tilde{t}) = E_1 \delta(\tilde{t} + \tilde{t}_1) + E_2 \delta(\tilde{t} + \tilde{t}_1 + \tilde{t}_2)$ (见图2蓝线), 即 $f(t) = f_1 \delta(\tilde{t} + \tilde{t}_1) + f_2 \delta(\tilde{t} + \tilde{t}_1 + \tilde{t}_2) = \frac{ed}{\omega} [E_1 \delta(\tilde{t} + \tilde{t}_1) + E_2 \delta(\tilde{t} + \tilde{t}_1 + \tilde{t}_2)]$ 。光脉冲在0时刻产生的响应可以通过式(17)和式(18)得到:

$$\begin{cases} \theta_{(1)}(0) = f_1 \dot{G}(\tilde{t}_1) + f_2 \dot{G}(\tilde{t}_1 + \tilde{t}_2) \\ \theta_{(3)}(0) = \frac{1}{6} \int_{-\infty}^0 d\tilde{\tau} G(-\tilde{\tau}) [f_1 \dot{G}(\tilde{\tau} + \tilde{t}_1) + f_2 \dot{G}(\tilde{\tau} + \tilde{t}_1 + \tilde{t}_2)]^3 \end{cases} \quad (19)$$

分别关闭第一个脉冲和第二个脉冲,仿照以上分析可以得到 θ 对一个脉冲的响应。将式(19)扣除掉只与一个脉冲相互作用的部分,即得到体系与两个脉冲均发生相互作用的部分 θ_m :

$$\theta_m(\tilde{t}_1, \tilde{t}_2) = \frac{1}{2} \int_{-\infty}^0 d\tilde{\tau} G(-\tilde{\tau}) [f_1^2 f_2 \dot{G}^2(\tilde{\tau} + \tilde{t}_1) \dot{G}(\tilde{\tau} + \tilde{t}_1 + \tilde{t}_2) + f_1 f_2^2 \dot{G}(\tilde{\tau} + \tilde{t}_1) \dot{G}^2(\tilde{\tau} + \tilde{t}_1 + \tilde{t}_2)]. \quad (20)$$

式(20)包含两个时间变量 \tilde{t}_1 和 \tilde{t}_2 ,对二者做二维傅里叶变换即得到体系的二维相干光谱。此外,同时利用数值方法模拟式(12),相关结果将在下一节介绍。

4 结 果

图 3 展示了体系的非线性响应。我们通过数值方法计算了 $\theta_m(\tilde{t}_1, \tilde{t}_2)$, 选取电场的形式 $E(\tilde{t}) = \cos(\tilde{t} + \tilde{t}_1) \exp\left[-\frac{(\tilde{t} + \tilde{t}_1)^2}{2}\right] + \cos(\tilde{t} + \tilde{t}_1 + \tilde{t}_2) \times \exp\left[-\frac{(\tilde{t} + \tilde{t}_1 + \tilde{t}_2)^2}{2}\right]$, 用以模拟实验上的单周期脉

冲。选择 $\gamma = 0.25$ 。其时域结果如图 3(a) 所示,信号沿 t_1 和 t_2 轴均存在振荡,并且随时间指数衰减,半衰期正比于 ω/γ 。进一步对图 3(a) 数据进行二维傅里叶变换,得到其二维相干光谱,如图 3(b) 所示。二维相干光谱上分布着清晰的 8 个峰,分别代表不同的信号。为了方便理解这些物理过程,借鉴描述量子系统的非线性光学过程的刘维尔路径这一语言^[11-12,14]。刘维尔路径描述了一个量子体系的密度矩阵的演化过程,不同的过程对应不同的路径,产生出不同的非线性信号。

图 3(b) 中蓝色圆圈标记了泵浦-探测信号,该信号正比于 $\exp(\pm i\omega t_1)$, 对应的刘维尔路径为

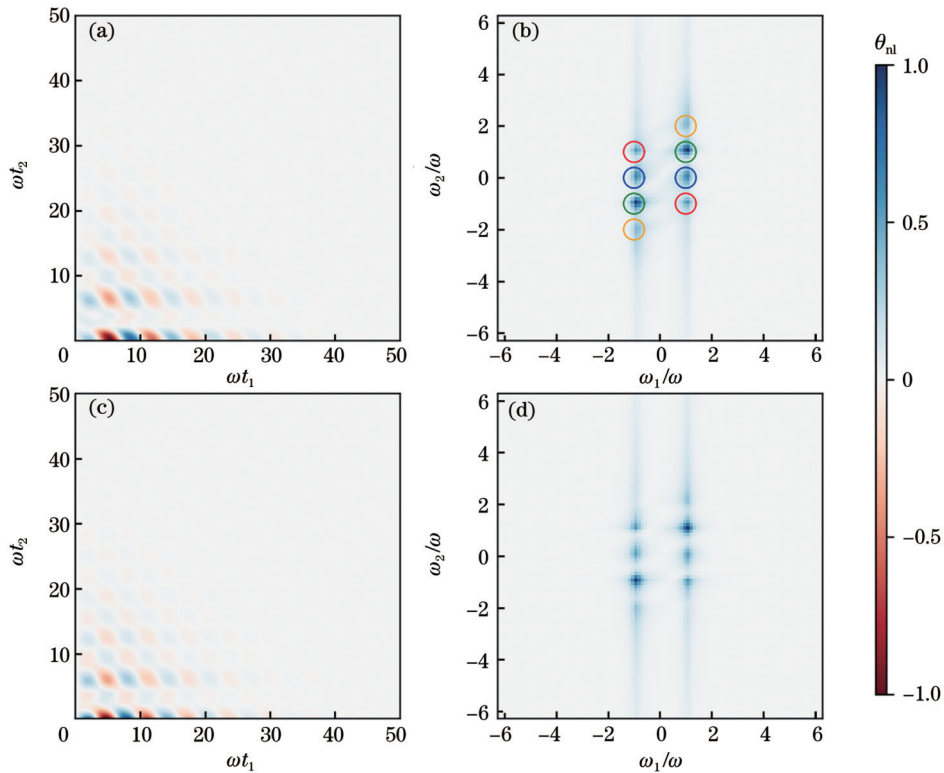


图 3 约瑟夫森等离子体模式的非线性响应。(a)由数值方法得到的 $\theta_m(t_1, t_2)$, 数据的最大值设置为 1; (b)(a)中数据二维傅里叶变换的绝对值,数据进行了归一化; (c)由格林函数方法得到的 $\theta_m(t_1, t_2)$; (d)(c)中数据二维傅里叶变换的绝对值

Fig. 3 Nonlinear response of Josephson plasmon. (a) $\theta_m(t_1, t_2)$ obtained from numerical method, with data being scaled such that the maximum is 1; (b) absolute value of 2D Fourier transform of (a), with data normalized; (c) $\theta_m(t_1, t_2)$ obtained from Green's function method; (d) absolute value of 2D Fourier transform of (c)

$$\begin{cases} |0\rangle\langle 0| \xrightarrow{E\rho E} |1\rangle\langle 1| \xrightarrow{E\rho} \exp(-\gamma\tilde{t}_2)|0\rangle\langle 1| \xrightarrow{\rho E} \exp[-\gamma(\tilde{t}_2 + \tilde{t}_1/2)] \exp(i\tilde{t}_1)|0\rangle\langle 0| \\ |0\rangle\langle 0| \xrightarrow{E\rho E} |1\rangle\langle 1| \xrightarrow{\rho E} \exp(-\gamma\tilde{t}_2)|1\rangle\langle 0| \xrightarrow{E\rho} \exp[-\gamma(\tilde{t}_2 + \tilde{t}_1/2)] \exp(-i\tilde{t}_1)|0\rangle\langle 0| \end{cases}, \quad (21)$$

式中: $\tilde{t}_{1,2} = \omega t_{1,2}$; $|0\rangle$ 表示体系的基态; $|1\rangle$ 表示体系产生一个等离子体激发。电场 E 能够激发一个约瑟夫森等离子体模式 $E|0\rangle \rightarrow |1\rangle$, 也可以诱导体系回到基态 $E|1\rangle \rightarrow |0\rangle$ 。更高能的态也可能在刘维尔路径中存在, 但因其衰减更快, 所以其对非线性响应的贡献很小。

红色圆圈标记了光子回波信号, 该信号正比于 $\exp[\pm i\omega(t_1 - t_2)]$, 其对应的刘维尔路径为

$$\begin{cases} |0\rangle\langle 0| \xrightarrow{E\rho} |1\rangle\langle 0| \xrightarrow{E\rho E} \exp(-\gamma\tilde{t}_2/2)\exp(-i\tilde{t}_2)|0\rangle\langle 1| \xrightarrow{\rho E} \exp[-\gamma(\tilde{t}_2 + \tilde{t}_1)/2]\exp[i(\tilde{t}_1 - \tilde{t}_2)]|0\rangle\langle 0| \\ |0\rangle\langle 0| \xrightarrow{\rho E} |0\rangle\langle 1| \xrightarrow{E\rho E} \exp(-\gamma\tilde{t}_2/2)\exp(i\tilde{t}_2)|1\rangle\langle 0| \xrightarrow{E\rho} \exp[-\gamma(\tilde{t}_2 + \tilde{t}_1)/2]\exp[-i(\tilde{t}_1 - \tilde{t}_2)]|0\rangle\langle 0| \end{cases} \quad (22)$$

当体系存在不均匀性时, 比如由于缺陷或杂质等原因, 导致电介质常数 ϵ 和约瑟夫森相互作用 J 存在不均匀性, 体系的线性光谱会存在不均匀展宽。光子回波信号能将这种不均匀展宽与激发的寿命以及体系的退相干导致的均匀展宽分离开, 从而得到激发的动力学信息。

绿色圆圈标记了“失相”信号, 该信号正比于 $\exp[\pm i\omega(t_1 + t_2)]$, 其对应的刘维尔路径为

$$\begin{cases} |0\rangle\langle 0| \xrightarrow{\rho E} |0\rangle\langle 1| \xrightarrow{\rho EE} \exp(-\gamma\tilde{t}_2/2)\exp(i\tilde{t}_2)|0\rangle\langle 1| \xrightarrow{\rho E} \exp[-\gamma(\tilde{t}_2 + \tilde{t}_1)/2]\exp[i(\tilde{t}_1 + \tilde{t}_2)]|0\rangle\langle 0| \\ |0\rangle\langle 0| \xrightarrow{E\rho} |1\rangle\langle 0| \xrightarrow{EE\rho} \exp(-\gamma\tilde{t}_2/2)\exp(-i\tilde{t}_2)|1\rangle\langle 0| \xrightarrow{E\rho} \exp[-\gamma(\tilde{t}_2 + \tilde{t}_1)/2]\exp[-i(\tilde{t}_1 + \tilde{t}_2)]|0\rangle\langle 0| \end{cases} \quad (23)$$

这一信号的衰减体现了体系的不均匀性, 信号衰减越快说明“失相”的效果越强, 体系的不均匀性越强。

橙色圆圈标记了双量子相干(2Q)信号, 该信号正比于 $\exp[\pm i\omega(t_1 + 2t_2)]$, 其对应的刘维尔路径为

$$\begin{cases} |0\rangle\langle 0| \xrightarrow{\rho EE} |0\rangle\langle 2| \xrightarrow{\rho E} \exp(-\gamma\tilde{t}_2)\exp(i2\tilde{t}_2)|0\rangle\langle 1| \xrightarrow{\rho E} \exp[-\gamma(\tilde{t}_2 + \tilde{t}_1/2)]\exp[i(\tilde{t}_1 + 2\tilde{t}_2)]|0\rangle\langle 0| \\ |0\rangle\langle 0| \xrightarrow{EE\rho} |2\rangle\langle 0| \xrightarrow{E\rho} \exp(-\gamma\tilde{t}_2)\exp(-i2\tilde{t}_2)|1\rangle\langle 0| \xrightarrow{E\rho} \exp[-\gamma(\tilde{t}_2 + \tilde{t}_1/2)]\exp[-i(\tilde{t}_1 + 2\tilde{t}_2)]|0\rangle\langle 0| \end{cases} \quad (24)$$

式中: $|2\rangle$ 代表体系中存在两个约瑟夫森等离子体集体激发。当体系中存在两个频率相近的模式时, 这一信号可以将两个模式的频率差别放大两倍, 使得不同模式更易区分。

进一步地, 我们应用格林函数方法计算了体系的非线性响应及其对应的二维相干光谱, 如图 3(c) 和图 3(d) 所示。为了解析的方便, 选取 $E(\tilde{t}) = \delta(\tilde{t} - \tilde{t}_2) + \delta(\tilde{t} + \tilde{t}_1 + \tilde{t}_2)$, 同时选取 $\gamma = 0.25$ 。解析结果与数值结果完全一致[图 3(a) 与图 3(c) 比较, 图 3(b) 与图 3(d) 比较], 说明脉冲的具体细节不会影响二维相干光谱的行为。

5 结 论

本文计算了层状高温超导体中约瑟夫森等离子体模式的二维相干光谱, 并解释了二维相干光谱的特征。这些特征对脉冲的具体细节不敏感, 从而有利于实验的检验。最近, 已经有实验利用泵浦-探测技术研究了 LBCO 中约瑟夫森等离子体模式的非线性响应^[28]。在此基础上, 通过增加探测光的强度, 实验上即可得到相关体系的二维相干光谱。

本文所使用的理论模型可在未来进一步拓展和改进, 从而更好地描述层状高温超导体中的约瑟夫森等离子体模式的二维相干光谱。首先, 在考虑的有效模型中, 我们忽略了相位在空间上的不均匀性。这是因为我们认为电场与材料的作用是空间均匀的并且忽略了体系对磁场的响应。如果引入空间自由度, 描述约瑟夫森等离子体的方程应当是 Sine-Gordon 方程^[26], 从

而带来一些新的效应。这些新效应对二维相干光谱的影响有待进一步研究。同时, Sine-Gordon 方程包含一类特殊的激发——孤子。这种激发已经被实验观测到^[31], 但其二维相干光谱特征尚不清楚。最后, 在推导约瑟夫森相位的运动方程时, 我们唯象地加入了耗散。为了更好地描述耗散过程, 需要从微观原理出发将耗散效应引入到模型中, 并分析它对约瑟夫森等离子体模式二维相干光谱的影响。

致谢 作者感谢王楠林、张思捷、董涛三位老师的有益讨论。

参 考 文 献

- [1] Orenstein J, Millis A J. Advances in the physics of high-temperature superconductivity[J]. Science, 2000, 288(5465): 468-475.
- [2] Norman M R, Pépin C. The electronic nature of high temperature cuprate superconductors[J]. Reports on Progress in Physics, 2003, 66(10): 1547-1610.
- [3] Jain M, Xia H, Yin G Y, et al. Efficient nonlinear frequency conversion with maximal atomic coherence[J]. Physical Review Letters, 1996, 77(21): 4326-4329.
- [4] Coldea R, Tennant D A, Wheeler E M, et al. Quantum criticality in an Ising chain: experimental evidence for emergent E8 symmetry[J]. Science, 2010, 327(5962): 177-180.
- [5] Gegenwart P, Si Q M, Steglich F. Quantum criticality in heavy-fermion metals[J]. Nature Physics, 2008, 4(3): 186-197.
- [6] Löhneysen H V, Rosch A, Vojta M, et al. Fermi-liquid instabilities at magnetic quantum phase transitions[J]. Reviews of Modern Physics, 2007, 79(3): 1015-1075.
- [7] Jepsen P U, Cooke D G, Koch M. Terahertz spectroscopy and imaging: modern techniques and applications[J]. Laser & Photonics

- Reviews, 2011, 5(1): 124-166.
- [8] Sirtori C. Bridge for the terahertz gap[J]. *Nature*, 2002, 417(6885): 132-133.
- [9] Köhler R, Tredicucci A, Beltram F, et al. Terahertz semiconductor-heterostructure laser[J]. *Nature*, 2002, 417(6885): 156-159.
- [10] 高润梅. 基于光学技术的太赫兹相干辐射源研究[J]. *中国激光*, 2008, 35(s2): 22-25.
Gao R M. Research into the terahertz coherent radiation source in view of optical technique[J]. *Chinese Journal of Lasers*, 2008, 35(s2): 22-25.
- [11] Mukamel S. Principles of nonlinear optical spectroscopy[M]. New York: Oxford University Press, 1995.
- [12] Hamm P, Zanni M T. Concepts and methods of 2D infrared spectroscopy[M]. Cambridge: Cambridge University Press, 2011.
- [13] Cundiff S T, Mukamel S. Optical multidimensional coherent spectroscopy[J]. *Physics Today*, 2013, 66(7): 44-49.
- [14] 李子龙, 万源. 强关联电子体系二维相干光谱的理论研究评述[J]. *物理学报*, 2021, 70(23): 230308.
Li Z L, Wan Y. A theoretical survey of two-dimensional coherent spectroscopy in strongly-correlated electronic systems[J]. *Acta Physica Sinica*, 2021, 70(23): 230308.
- [15] Hahn E L. Spin echoes[J]. *Physical Review*, 1950, 80(4): 580-594.
- [16] Wan Y, Armitage N. Resolving continua of fractional excitations by spinon echo in THz 2D coherent spectroscopy[J]. *Physical Review Letters*, 2019, 122(25): 257401.
- [17] Choi W, Lee K H, Kim Y B. Theory of two-dimensional nonlinear spectroscopy for the Kitaev spin liquid[J]. *Physical Review Letters*, 2020, 124(11): 117205.
- [18] Nandkishore R M, Choi W, Kim Y B. Spectroscopic fingerprints of gapped quantum spin liquids, both conventional and fractonic[J]. *Physical Review Research*, 2021, 3(1): 013254.
- [19] Li Z L, Oshikawa M, Wan Y. Photon echo from lensing of fractional excitations in Tomonaga-Luttinger spin liquid[J]. *Physical Review X*, 2021, 11(3): 031035.
- [20] Negahdari M K, Langari A. Nonlinear response of the Kitaev honeycomb lattice model in a weak magnetic field[J]. *Physical Review B*, 2023, 107(13): 134404.
- [21] Hart O, Nandkishore R. Extracting spinon self-energies from two-dimensional coherent spectroscopy[J]. *Physical Review B*, 2023, 107(20): 205143.
- [22] Parameswaran S, Gopalakrishnan S. Asymptotically exact theory for nonlinear spectroscopy of random quantum magnets[J]. *Physical Review Letters*, 2020, 125(23): 237601.
- [23] Gao Q, Liu Y, Liao H J, et al. Two-dimensional coherent spectrum of interacting spinons from matrix product states[J]. *Physical Review B*, 2023, 107(16): 165121.
- [24] Sim G, Knolle J, Pollmann F. Nonlinear spectroscopy of bound states in perturbed Ising spin chains[J]. *Physical Review B*, 2023, 107(10): L100404.
- [25] Hamm P, Meuwly M, Johnson S L, et al. Perspective: THz-driven nuclear dynamics from solids to molecules[J]. *Structural Dynamics*, 2017, 4(6): 061601.
- [26] Laplace Y, Cavalleri A. Josephson plasmonics in layered superconductors[J]. *Advances in Physics: X*, 2016, 1(3): 387-411.
- [27] Dubroka A, Rössle M, Kim K W, et al. Evidence of a precursor superconducting phase at temperatures as high as 180 K in $\text{RBa}_2\text{Cu}_3\text{O}_{7-\delta}$ (R=Y, Gd, Eu) superconducting crystals from infrared spectroscopy[J]. *Physical Review Letters*, 2011, 106(4): 047006.
- [28] Zhang S J, Liu Q M, Sun Z, et al. Out-of-plane nonlinear optical responses of superconducting cuprates detected by terahertz pump-terahertz probe spectroscopy[EB/OL]. (2022-02-28) [2023-02-03]. <https://arxiv.org/abs/2202.13858>.
- [29] Tinkham M. Introduction to superconductivity[M]. 2nd ed. Mineola: Dover Publications, 2004.
- [30] Wen X G. Quantum field theory of many-body systems: from the origin of sound to an origin of light and electrons[M]. Oxford: Oxford University Press, 2004.
- [31] Dienst A, Casandru E, Fausti D, et al. Optical excitation of Josephson plasma solitons in a cuprate superconductor[J]. *Nature Materials*, 2013, 12(6): 535-541.

Theoretical Survey of Terahertz Two-Dimensional Coherent Spectroscopy of Josephson Plasmon Mode in Layered High-Temperature Superconductor

Li Zilong^{1,2}, Wan Yuan^{1,2,3*}

¹Key Laboratory of Condensed Matter Theory and Computation, Institute of Physics, Chinese Academy of Sciences, Beijing 100190, China;

²School of Physical Sciences, University of Chinese Academy of Sciences, Beijing 100049, China;

³Songshan Lake Materials Laboratory, Dongguan 523808, Guangdong, China

Abstract

Objectives As a newly developed ultrafast optical spectroscopy, terahertz two-dimensional coherent spectroscopy (2DCS) has become a promising method to characterize the physical properties of optical excitations in various materials. It utilizes two or more THz pulses to detect nonlinear responses of materials, thereby incorporating multiple frequency variables. Experimentally, it has uncovered a host of interesting phenomena in quantum wells, electronic glasses, and superconductors. In this work, we theoretically investigate the 2DCS of the Josephson plasmon mode in layered high-temperature superconductors.

Layered high-temperature superconductors consist of alternating superconducting and insulating layers. The adjacent superconducting-insulating-superconducting layers form a Josephson junction. Consequently, the layered high-temperature superconductors possess a nonlinear mode, known as “Josephson plasmon mode”. The Josephson plasmon mode arises from Josephson tunneling of Cooper pairs across the neighboring superconducting layers separated by insulating block layers.

In this work, we compute the 2DCS of the Josephson plasmon mode and analyze the features therein. We expect that our findings will provide the theoretical basis for the future 2DCS experiments on layered high-temperature superconductors.

Methods We begin with a semiclassical effective model of layered high-temperature superconductors. We derive and solve

numerically the equation of motions of the Josephson mode coupled to the electrical field. Fourier transforming the time-domain data yields 2DCS. Meanwhile, assuming that the electrical field is weak, we are able to solve the equation of motion analytically by using the perturbation theory. Finally, we associate the peaks in the two-dimensional spectrum with the Liouville paths and clarify the response process in detail.

Results and Discussions Figure 3 shows the 2DCS of the Josephson plasmon mode. The numerical results [Figs. 3(a) and 3(b)] are found to be consistent with the analytical results [Figs. 3(c) and 3(d)]. In the time domain [Figs. 3(a) and 3(c)], the signals decay exponentially with increasing t_1 or t_2 . The decay rate is proportional to the resistance of the Josephson junctions in layered high-temperature superconductors, γ . Meanwhile, the signal oscillates with the frequency of the Josephson plasmon mode, ω . In the frequency domain [Figs. 3(b) and 3(d)], the 2DCS exhibits eight peaks. In Fig. 3(b), the blue circles label the pump-probe peaks. The red circles label the photon echo peaks, which can help to separate the homogeneous broadening and inhomogeneous broadening. The green circles label the dephasing peaks. The orange circles label the two-quantum (2Q) peaks, which correspond to the simultaneous excitation of two plasmon mode quanta.

Conclusions We have investigated the 2DCS of Josephson plasmon mode in layered high-temperature superconductors. Our findings reveal that the 2DCS contains various peaks, including pump-probe peaks, photon echo peaks, dephasing peaks, and 2Q peaks. We have also clarified their origins by associating these peaks to the various optical transition processes.

We envision that our model may be extended and improved in various aspects. Firstly, by adding the spatial degrees of freedom, the corresponding equation of motions would become sine-Gordon equation. Sine-Gordon equation hosts a specific excitation: soliton. Soliton has been detected in experiments but its 2DCS signature is still unclear and requires further investigation. Secondly, in deriving the equation of motion, the resistance is introduced phenomenologically. It would be interesting to derive the dissipative term from the first principles.

Key words terahertz; terahertz two-dimensional coherent spectroscopy; Josephson plasmon mode; layered high-temperature superconductor